Pelvic organ prolapse meshes: Can they preserve the physiological behavior?

Annie Morch, Guillaume Doucède, Pauline Lecomte-Grosbras, Mathias Brieu, Chrystèle Rubod, Michel Cosson

Pelvic organ prolapse meshes: can they preserve the physiological behavior ?

Annie Morch[a], Guillaume Doucède[b,c], Pauline Lecomte-Grosbras[a], Mathias Brieu[a,d], Chrystèle Rubod[a,b,c], Michel Cosson[a,b,c,*]

[a] *Univ. Lille, CNRS, Centrale Lille, UMR 9013- LaMcube - Laboratoire de Mécanique, Multiphysique, Multi-échelle, F-59000 Lille, France*
[b] *Service de chirurgie gynécologique - CHU Lille - F-59000 Lille, France*
[c] *Université de Lille - Faculté de Lille - F-59000 Lille, France*
[d] *California State University - Los Angeles - College Engineering - Computer Science, and Technology Dept. Mechanical Engineering.*

Abstract

Implants for the cure of female genital prolapse still show numerous complications cases that sometimes have dramatic consequences. These implants must be improved to provide physiological support and restore the normal functionalities of the pelvic area. Besides the trend towards lighter meshes, a better understanding of the *in vivo* role and impact of the mesh implantation is required.

This work investigates the mechanical impact of meshes after implantation with regards to the behavior of the native tissues. Three meshes were studied to assess their mechanical and biological impact on the native tissues. An animal study was conducted on rats. Four groups (n = 17/group) underwent surgery. Rats were implanted on the abdominal wall with one of the three polypropylene knitted mesh (one mesh/group). The last group served as control and underwent the same surgery without any mesh implantation.

Post-operative complications, contraction, mechanical rigidities, and residual deformation after cyclic loading were collected. Non-parametric statistical comparisons were performed (Kruskal-Wallis) to observe potential differences between implanted and control groups.

Mechanical characterization showed that one of the three meshes did not alter the mechanical behavior of the native tissues. On the contrary, the two others drastically increased the rigidities and were also associated with clinical complications. All of the meshes seem to reduce the geometrical lengthening of the biological tissues that comes with repetitive loads.

Mechanical aspects might play a key role in the compatibility of the mesh *in vivo*. One of the three materials that were implanted during an animal study seems to provide better support and adapt more properly to the physiological behavior of the native tissues.

1. Introduction

Pelvic organ prolapse (POP) characterized by the descent of one or more pelvic organs into the vagina, comes with troublesome symptoms (urinary incontinence, bulge feeling, chronic pain,...). They cause serious discomfort and can dramatically impact the everyday life of the patient. Treatments are often required to restore the normal mobilities of the pelvic area and improve the patients life.

Surgical treatments may be required to restore the normal anatomy and mobilities of the pelvic area and improve the patient's quality of life. During the past decades, the surgical procedure developed: instead of the traditional use of the native tissue and re-conformation of the pelvic system, surgical procedure trended to use synthetic mesh [1, 2]. These meshes are usually knitted textiles that are placed between the prolapsed organ and the vagina to restore the pelvic physiology and limit the extreme mobilities of the pathology.

*Corresponding author : michel.cosson@chru-lille.fr

While the use of synthetic prostheses seems to reduce the recurrence rate observed with traditional surgery [3], their use remains controversial. Post-operative complications cases are frequent [4, 5] and lead to drastic FDA recommendations. Vaginal meshes have been withdrawn from the US market. Some are still used in Europe and worldwide for stress urinary incontinence and through laparoscopic implantation for prolapse.

This urged the need to better understand the role of these meshes and the impact of their implantation on the native tissues. The implantation of a mesh may cause an immune response of the body. In pathological cases, this immune response may be extreme, leading to excessive inflammation and fibrosis. The inflammatory process overreacts and is responsible for the contraction, pain, and sometimes exposure of the mesh through the native tissues [6–8]. The origin of this pathological immune response is believed to be multi-factorial: features such as the polymer yarn, mesh coating, pore shape or size, mechanical rigidity, etc, can trigger an overreaction of the immune system.

Most specifications about the meshes concern its biocompatibility properties [9, 10]. Non-resorbable meshes are preferably macro-porous textiles, mostly knitted from polypropylene monofilament yarns. There are usual recommendations regarding the choice of a hypoallergenic, non-carcinogenic material but also toward a mesh that limits the inflammatory response and prevents infection or adhesion to the tissues.

Several studies suggested that the large number of complications and the poor host-integration might be due to a greater mesh rigidity prior to implantation [11] or a mismatch between the mechanical properties of the mesh and the native tissues [12, 13]. To our knowledge, there is barely any specification about the mechanical properties of the mesh, whether before implantation, but most importantly after implantation once colonized by neo-tissue, in its *in vivo* state. This could, however, be a key parameter for the success of these meshes: the mesh, once implanted and colonized by scar tissue, should restore the physiological mechanical behavior of the native tissues.

To improve the integration of prostheses and limit post-operative complications, mechanical specifications on the *in vivo* behavior of the mesh seem mandatory: specifications should apply to the mechanical behavior of the mesh after it is implanted and colonized by scar tissue rather than before the implantation, without being colonized by the tissue. Once implanted, the prosthesis will integrate into the body and form a biological composite with the native and scar tissue, which is supposed to ensure the normal physiological functions of the pelvic system and limit pathological mobilities.

After its implantation, the mesh forms with the native and scar tissues a biological composite that remains yet poorly known. It seems however difficult to predict the biomechanical compatibility of a mesh directly from the raw mesh properties. There is an urgent need to better understand the role of these meshes and the impact of their implantation on the native tissues. In the literature, numerous works already studied mesh implantation in animal models looking at mechanical and histological features [11, 14–17]. Liang et al. [11] and Feola et al. [14] studied respectively the histomorphological and tissue composition aspects and biomechanical properties of the same commercial meshes. Their conclusions head toward the same conclusion that the stiffest mesh has a negative impact regarding tissue composition and mechanical properties. The impact of the mesh weight was assessed in different studies [16, 17] highlighting the benefits of the lighter mesh in long term considerations: lesser foreign material is implanted and some meshes can reproduce the mechanical behavior of the native tissues in specific directions. These studies proposed interesting insights about the effect of mostly commercial meshes after implantation regarding specific histological or mechanical parameters. We want to provide a comprehensive study that correlates raw textiles to their *in vivo* impact in terms of mechanical properties but also clinical complications in comparison with the native tissues. That would help to assess the choice of an optimal mesh with regards to its final purpose, here the cure of pelvic organ prolapse.

For this study, three meshes were implanted in an animal model to investigate, with regards to their raw properties, their impact on the mechanical behavior of the biological composite (BC) made of native tissues, mesh and scar tissues after implantation.

First, we detail the animal model and the textiles implanted during this study. We then specify the choice of the mechanical parameters that will be used to evaluate the impact of the implantation of the prostheses. The second section presents our main results, in terms of mechanical impact on the native tissue behavior and clinical observations following the implantation and healing. In the last part of the present

paper, we will discuss the validity and limitations of the results.

2. Material and method

2.1. Textile implants

Three knitted textiles A, B, and C were designed and manufactured by DYLCO (Bertry, France), with a 80 µm diameter polypropylene yarn.

Like the biological soft tissues, meshes present a non-linear behavior: average rigidities at small and large deformations are presented in Table 1 along with the textiles' physical and geometrical features. These average results are obtained using 5 test specimens.

Name	Surface weight (g/m^2)	Pore size (mm) Diameter	Rigidity (N) Initial	Rigidity (N) Final
A	28	1.30 ± 0.07	0.24 ± 0.03	2.54 ± 0.04
B	18	2.16 ± 0.04	0.092 ± 0.002	1.85 ± 0.07
C	13	3.87 ± 0.10	0.058 ± 0.007	1.16 ± 0.12

Table 1: Average properties of the textiles A, B, and C: surface weight, largest pore dimension and rigidities. Values are averaged from five tested samples.

Surface weight is measured according to norm NF-EN-12127. To measure the pore size, textile samples are dyed in a bright color (white or silver painting), pictured with a macro-lens (Canon EF 100mm f/2.8 Macro USM) on a dark background. A graduated marker on the picture helps to get the pixel to mm correspondence. Images are then processed with the software ImageJ. For each textile, macropores are identified as illustrated in Figure 1. Pores are approximated by an ellipse of the small and large axis a and b. The diameter of the equivalent circle is then quantified as $d = \sqrt{ab}$. Interstitial pores and smaller pores were not quantified.

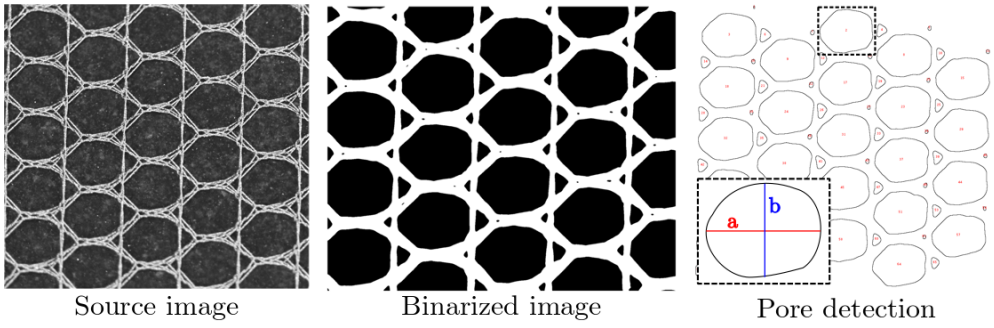

Figure 1: Pore size evaluation. The source image is binarized and pore contours detected.

All three meshes present distinct densities, pore size, and rigidities. Meshes A and B have a rather hexagonal pore type, while mesh C shows large round pores, as shown in Figure 2.

The mechanical properties of the plain textile are obtained following textile testing standards (NF-EN-13494-1). Five samples of 20 cm long and 5 cm width are tested under uniaxial tension in the warp direction. Tests were performed at a displacement speed of 20 mm/min on an electromechanical tensile testing machine (Instron). The sample is tightened between grips equipped with rubber plates to avoid slipping. The force is measured with a 2.5 kN loadcell. The deformation is computed as the clamp to clamp's distance ratio.

The average mechanical behavior of the knitted mesh is approximately bi-linear, as shown in Figure 3. Because of their nature (knitted, very porous textile), meshes are closer to structures than to a plain

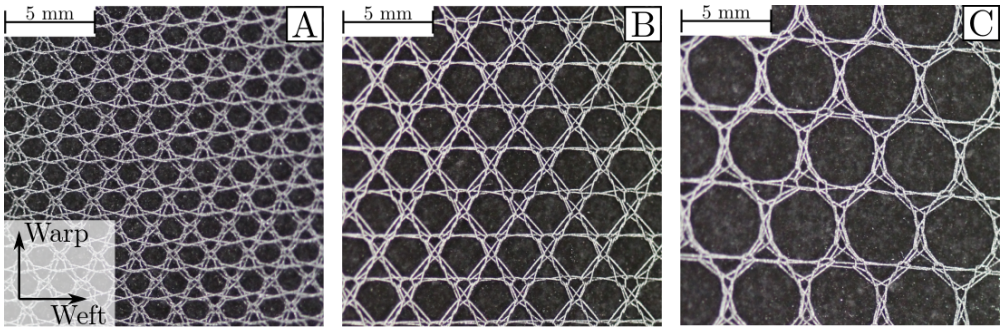

Figure 2: Close-up view of the architectures of textile A, B and C

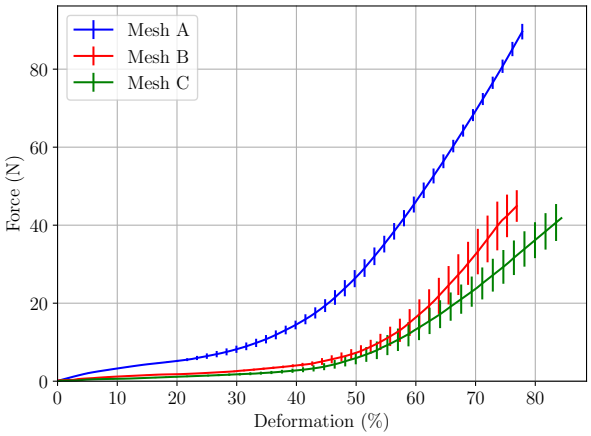

Figure 3: Average force vs deformation behavior of the three meshes under uniaxial traction following warp direction. Five samples of each mesh were tested. Error bars display the standard deviation

material. Computing the stress within such a flat porous structure proves difficult. For this reason, a different mechanical characterization was performed on the raw mesh and biological composites.

Rigidities under small and large deformations are respectively computed as the slope in the first 20% and the last 20% of deformations; to have a rough approximation of the overall behavior of the mesh. The ranges of identification were fixed arbitrarily and approximately correspond to the two linear areas in the mechanical response [18].

2.2. Animal study

Sixty-eight rats were divided into four groups: a control group, that went through a sham surgery, and three implanted groups, that were implanted with one textile. They are called Group A, B, or C, according to the implanted textile reference.

This protocol has been approved by the local ethics committee (Comité d'Ethique en Expérimentation Animale Nord-Pas-de-Calais - CEEA 75).

The mesh consisted of a 7 cm long and 5 cm large textile rectangle, whose longer side was aligned with the warp direction of the textile. During the implantation, it was centered on the abdominal wall, with the long side corresponding with the craniocaudal direction [19, 20]. The control group's rat underwent the same surgery without the implantation of a mesh: the surgery was assumed to favor the development of scar tissues on the abdominal wall.

Three months after implantation, to ensure stabilized healing [19, 20], the rats were euthanized. The abdomen was opened along the implantation scar. The BC was resected *en bloc*. The control group was

explanted following the same protocol.

Complications were classified by severity during the healing and at the time of sacrifice: hematoma, infection, mesh exposition, or erosion. Mesh contraction is often believed to cause pain and discomfort to the patient [21]. The shrinkage of the mesh was assessed by evaluating the contraction of the mesh prior to harvesting. It was estimated by measuring the length and width between the sutures at the time and after implantation and computing the current to initial area ratio of the mesh.

2.3. Mechanical characterization

Mechanical properties are evaluated by performing cyclic uniaxial tensile tests immediately after harvesting, with an in-house developed testing machine, called Biotens [19], shown in Figure 4-a).

A 6 cm long and 2 cm wide sample is punched in the abdominal wall, centered on the linea alba. The initial thickness, e_0, is measured while placing the sample between two glass slides under a comparator. The sample dimensions are measured before testing to compute the stress from the force measurement: l_0 and e_0 respectively the initial width and thickness in mm.

In a previous study [19], we were able to gather preliminary information about the mechanical behavior of the control rat abdominal wall. It appeared that beyond 40% of deformation most of the samples show signs of damage or rupture. Thus, to study the damage appearance and/or growth, we decided to study the permanent strain induced by damage within the physiological range of strain on the biological composite. We, therefore, characterized the behavior under cyclic loads, observing the permanent strain after each unloading phase, beyond 40% of strain.

Cyclic uniaxial tension tests are performed at a displacement rate of 5 mm/min, corresponding to an average 0.03 s^{-1} strain rate. Force is measured with a 100 N loadcell (sensitivity: 0.02 N). The stress is computed as $\sigma = \dfrac{F}{e_0 l_0}$ from the force measurement F and l_0 and e_0 respectively the initial width and thickness in mm. Elongation is computed as the ratio between the current L and initial L_0 clamp-to-clamp distances.

The sample is stretched at increasing deformation levels, set to 10, 25, and 40%, as shown in Figure 4-b). Once the deformation threshold is attained, the sample is unloaded to 0.1 N. Three cycles are performed at the first three deformation stages and only two at the last one (40%). Above the last deformation level, the samples tend to severely damage or break, therefore a monotonic uniaxial tension follows the two last cycles.

The mechanical response is non-linear, hyperelastic and assumed isotropic. It can be modeled with a Yeoh second order model [22]. The strain energy density W depends on the right Cauchy-Green tensor $\mathbf{C}$:

$$W = C_0(I_1 - 3) + C_1(I_1 - 3)^2 \tag{1}$$

using two coefficient C_0 and C_1 and the first invariant $I_1 = Tr(\mathbf{C})$, with Tr the trace operator.

Assuming the incompressibility of the tissues due to their water content, the Cauchy-Green tensor in simple tension is diagonal: $\mathbf{C} = diag(\lambda, \frac{1}{\sqrt{\lambda}}, \frac{1}{\sqrt{\lambda}})$, where λ is the elongation.

The stress σ depends therefore of the elongation λ with respect to:

$$\sigma = 2(\lambda - \frac{1}{\lambda^2}) \left(C_0 + 2C_1(\lambda^2 + \frac{2}{\lambda} - 3) \right) \tag{2}$$

C_0 denotes the rigidity at small strain while C_1 characterizes the rigidity at large strain, the tangential behaviors are illustrated in Figure 4-c). The parameters are optimized for each dataset by minimizing the squared error between the experimental and modeled stress using a linear least-square algorithm available in the Python Scipy library [23].

The toe region of the stress-strain curve is characterized by low efforts at small displacement. The comfort zone limit delimits the areas of low and high stiffness. For human vaginal tissues, it is considered to be representative of everyday physiological conditions [13, 24]. In the large stiffness zone, stresses become important and are related to rarer physiological or traumatic events. If the comfort zone is shrunk, with the implantation of a mesh, for example, stresses would be higher at deformation corresponding to physiological

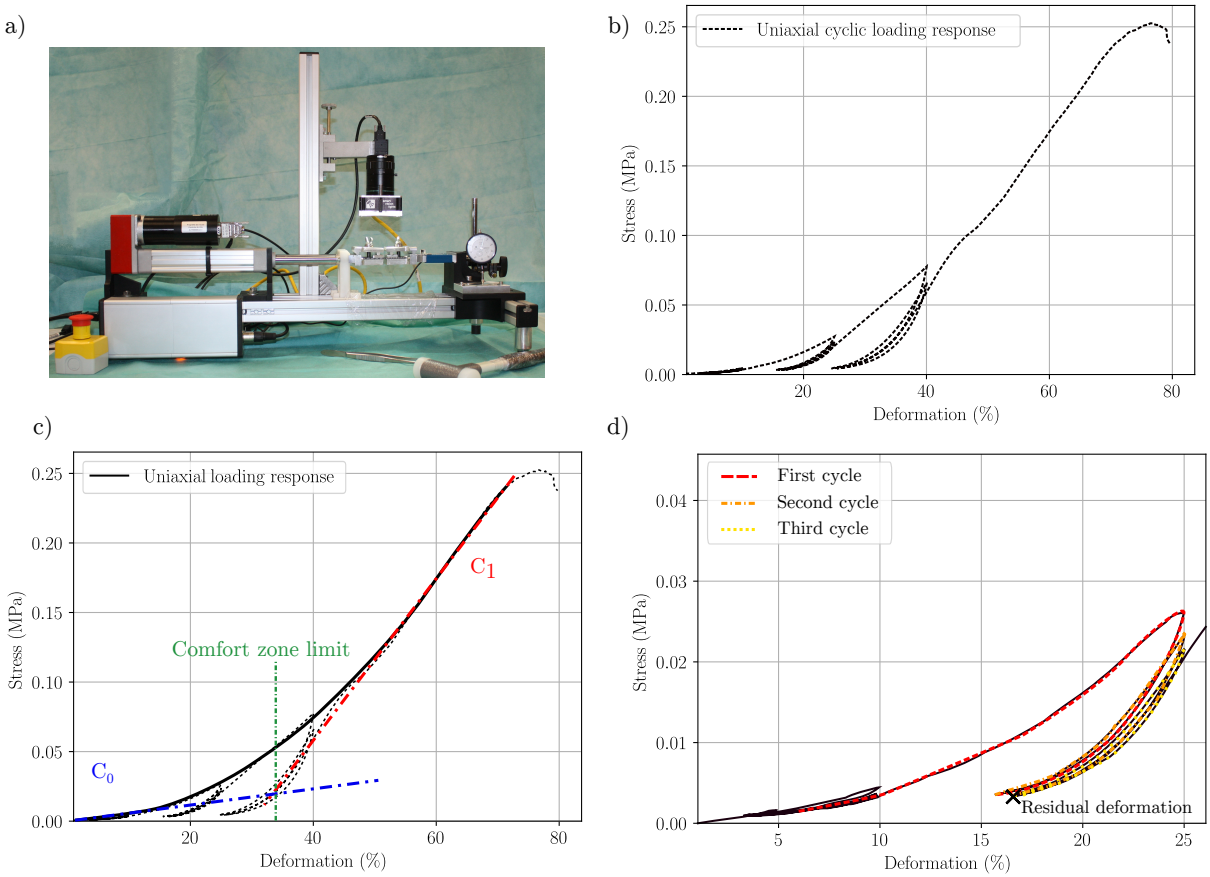

Figure 4: a) Mechanical tensile testing machine Biotens (internal development), b) Typical mechanical response in uniaxial cyclic loading, c) Monotonic uniaxial behavior retrieved from the cyclic response. The preponderance of C_0 and C_1 are indicated in the graph. The limit of the comfort zone is defined at the intersection of the initial and final tangent. d) Close-up view of the 3 cycles at 25% deformation and identification method of the residual strain.

situations, and may, therefore, cause pain to the patient. It is difficult in the present study to decide if the toe region is associated with the comfort of the animal. However, the conservation of the toe region could be a relevant insight into the compatibility of the mesh.

In the present work, the comfort zone limit is determined as the deformation obtained at the intersection of the initial and final tangent to the experimental curve [25]. The comfort limit deformation is found at the intersection of the initial and final linear tangent to the experimental curves. They are respectively obtained by linear regression on the first and last 10% of deformation.

The residual deformation is increasing with the number of cycles performed at one level. They are therefore identified after the last unloading at each deformation level when the stress reaches a minimum value of 0.004 MPa, as illustrated in Figure 4-d). It characterizes the geometrical irreversible lengthening of the sample occurring after several loadings.

2.4. Statistics

The median and interquartile range (IQR) are presented to handle the non-normal distribution of the mechanical results. Statistical comparisons are performed with Python Scipy (1.3.0) [23]. All groups are first compared with a Kruskal-Wallis test considering rigidities and comfort zone. In the case of a significant p-value, a Mann-Whitney-U *post-hoc* test is run for pairwise comparisons to the control group. A p-value of

less than 0.05 is considered significant. The measure of the residual deformation is considered as a qualitative value: it is difficult to estimate accurately. Therefore statistical comparisons between groups regarding this parameter were not performed.

3. Results

3.1. Clinical observations

Group A presented three cases of severe mesh exposures. Given the severity of the exposure, the abdominal walls of the three affected rats were not explanted. The other groups, B and C, did not present any exposure case. Five and nine cases of hematoma were noticed in groups B and C respectively during the three months post-surgery. All were resorbed by the time of the explantation. Retraction are reported in Table 2. The median values remain in the same range, around 30% in the area.

	Area contraction (IQR)(%)	Exposition	Complications
A	30.2 (17.8)	3	
B	30.7 (10.3)	0	5 hematomas (resorbed at the time of explantation)
C	36.7 (27.8)	0	9 hematomas (resorbed at the time of explantation)

Table 2: Clinical observations and median mesh contraction.

However, locally, four cases of extreme contraction were observed in group C. Figure 5 shows a case of extreme local contraction. The mesh was fixed at the four corners, which limited the contraction along the edges. In the central area, far from the borders, mesh C happened to severely shrink with a longitudinal contraction superior to 50% in the linea alba area where the mechanical sample is cut. The mesh implant aspect was extremely stiff in these cases. Cases of severe contraction or exposure were therefore not mechanically tested.

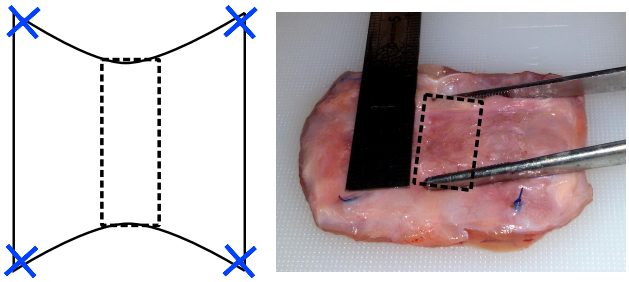

Figure 5: Extreme contraction case: the mesh length in the middle area is less than 50% of its original length

3.2. Apparent rigidities

Table 3 reports the evolution of the rigidities according to the animal groups. Figure 6 illustrates the dispersion of the mechanical results, using the identified mechanical parameters.

Global comparisons were not able to tell any significant differences for the rigidity at small deformations C_0 ($p = 0.3$) but detected significant one for the rigidity at large deformations C_1 ($p = 3.10^{-2}$).

The implantation of mesh A or C seems to significantly increase the rigidity in large deformation ($p^{Control/A} = 2.10^{-2}$ and $p^{Control/C} = 1.10^{-2}$). Mesh B was not significantly different from Control under large deformations ($p^{Control/B} = 0.4$). It may preserve physiological rigidities.

3.3. Comfort zone

Table 3 presents the comfort deformation limit for the four groups. The global comparison shows a significant difference between the groups ($p = 6.10^{-7}$).

Unlike mesh B, mesh A and C on the contrary significantly shifted the inflection point to the left, hence reduced the physiological comfort zone as identified with the control group.

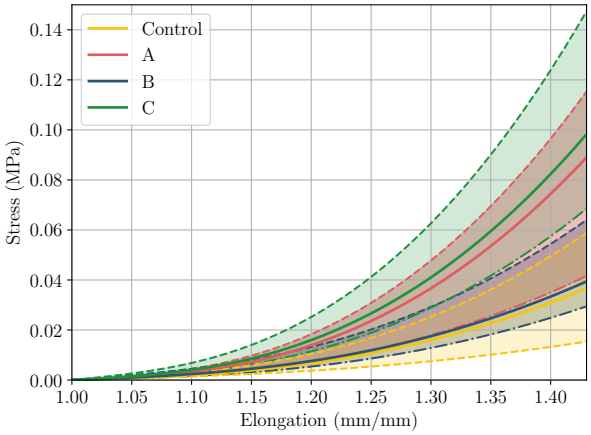

Figure 6: Mechanical behaviors of the observation groups. The median behavior is plotted in full lines, the variability range is filled between two dashed lines respectively the first and third quartiles.

Name	C_0 (kPa) Median (IQR)	C_1 (kPa) Median (IQR)	Comfort zone limit (deformation(%)) Median (IQR)
Control	2.3 (1.4)	31 (15)*,†	37.5 (10.9)*,†
A	3.4 (5)	59 (55)*	17.1 (6.37)*
B	4.7 (5.7)	26 (26)	33.9 (21.2)
C	3.9 (1.8)	47 (35)†	16.9 (17.2)†

Table 3: Mechanical properties of the groups. Median and interquartile range ($Q_3 - Q_1$) of rigidities at small and large deformations and comfort deformation are given. Symbols $\star$ and † show a significant difference between the two groups.

3.4. Residual strain

Figure 7 displays the mean value of the residual deformation ratio after cycling at 10, 25% and 40% of deformation. The ratio is computed as the residual deformation of the group to the residual deformation of the control group. Table 4 presents the median and interquartile range of the residual deformation of each group.

Below 10% of deformation, the evaluation of the residual deformation remains difficult due to large variation. Comparing results obtained on the control samples and the mesh composites above that deformation level highlights the added value of the mesh. Mesh A limited the progression of the residual deformation compared to the control abdominal wall. To a lesser extent, the two other meshes also seemed to have a beneficial impact on the evolution of the residual strain.

Deformation level	10%	25%	40%
	Median (IQR)	Median (IQR)	Median (IQR)
Control	5.0 (3)	16.5 (4.6)	24.3 (3.8)
A	5.9 (1.4)	11.0 (2.9)	17.7 (1.9)
B	6.4 (2.0)	15.0 (2.5)	21.0 (1.8)
C	6.5 (1.5)	14.5 (2.7)	22.5 (2)

Table 4: Median and interquartile range (Q3 -Q1) of the residual deformation.

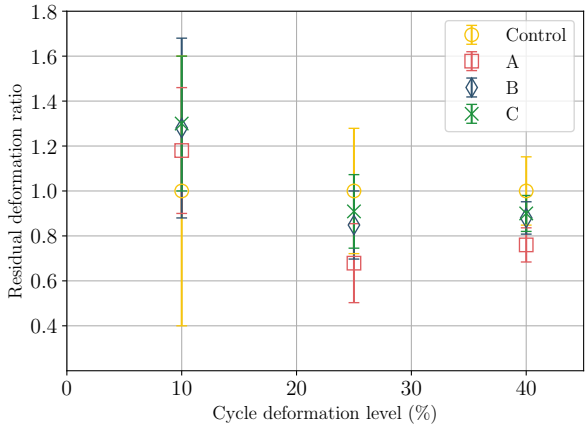

Figure 7: Evolution of the average residual deformation ratio after cycles at 10, 25 et 40% deformations according to the observation group.

4. Discussion

The impact of mesh implantation was assessed regarding clinical but mostly mechanical observations: complication cases, mechanical parameters in uniaxial tension, comfort zone, and residual deformation.

Clinical outcomes evaluation consisted of the quantification of major complications and mesh contraction. They gave relevant insights about the compatibility of the meshes. Serious cases of contraction happened after the implantation of mesh C, that were not observed with the two other meshes. The poor integration of mesh C suggests its lack of physiological compatibility. Mesh implants seem to protect the native tissues from geometrical lengthening, that usually appears over repeated solicitations. Depending on the type of the mesh, we observed an increase in the rigidities under large deformation of the BC with mesh A or C in comparison to the native tissues alone. This rigidity rise was also combined with a reduction of the comfort zone. On the contrary, mesh B did not impact those mechanical properties, preserving the physiological range of deformation of the native tissues. Our limited observations still suggest that the modification of the mechanical properties were often associated with severe complications.

The urogynecological implant market trends toward ultra-weight meshes, that are expected to provide improved bio-compatibility [26]. Mesh B is a hexagonal pore shape lighter version of mesh A which proved to provide better *in vivo* integration. Mesh C presents round and larger pores. Despite being lighter than A and B, its implantation led to extreme retraction cases and a significant change in the mechanical properties of the BC. Recently Lake et al. [27] explored the impact of the mesh physical properties on the host integration quantifying histological and mechanical effects. With much heavier meshes (above 38 g/m^2), they showed that the pore size and shape of the mesh seem to impact the host integration more than its density. The knitted design or architecture is responsible for the textile's ability to deform. The mesh's architecture allows it to rearrange and stretch at low forces with respect to the physiological mobilities and deformations of the native tissues. It could be interesting, in a similar approach to Röhrnbauer and Mazza [28] to relate the geometry to the raw mechanical properties. The link between the mesh raw properties and its *in vivo* integration is not straightforward and would require further investigations to understand the impact of the pore geometry.

Mesh's *in vivo* integration is a complex phenomenon to study as it might rely on both the mechanical but also the physical aspects of the mesh. Textile meshes are basically structures. Their nature kept us from comparing the raw mechanical properties to the biological composite's ones. During a mechanical test on a knitted textile, one observes a quite bilinear response of the force with respect to the deformation. In the beginning, one sees a structure response: the pores deforms while the yarn sections tend to realign with the traction direction. Once yarns are realigned, the yarn material (polypropylene here) defines the

rigidity of the mesh. There are therefore two phases: a structure and a material one, that both tend to disappear when looking at the biological composite. The latter is indeed closer to a plain material than the former. Moreover, if we were to apply the mechanical testing conditions of the biological composite, the cyclic testing would take place either during the structure response or the material one of the plain mesh. This raises questions in terms of mechanical testing: how relevant is the comparison between the raw textile vs biological composites. This is why we did not apply nor compare the same mesh before and after implantation in terms of mechanical parameters.

The two meshes, A and C, even if they were completely different in their raw state, provoked severe complications and significantly changed the mechanical response of the composite. On the contrary, mesh B did not seem to impact the mechanical behavior of the native tissues: the mesh-tissue composite behaved in a similar way to the native tissues. It seems counter-intuitive to imagine that the addition of a rigid element, the mesh, would have no effect on the rigidity of the BC. Similar observations were reported by Melman et al. [29] after the implantation of meshes in a porcine hernia model. In a rat model, the study by Ulrich et al. [30] observed the stiffness with a ball-burst test of the native abdominal wall and mesh-tissue complex issued from the implantation of a mesh. The mesh-tissue-complex with the Restorelle mesh was also revealed to be as stiff as the native tissues.

The cyclic data displayed the impact of the mesh as all implanted groups presented lower residual deformation growth than the native tissues. For larger deformation, the role of the mesh appears to be more significant. Although those data are rather quantitative, they compare well with the study of Ulrich et al. [30]. Market meshes were implanted on rats' abdominal wall and tested after 30 and 90 days following implantation. In a comparable manner, the implants with meshes seem to significantly lower the residual deformation when compared to the control group without mesh.

The present work lacks information about the biological aspects of the mesh implantation. The explant was harvested *en-bloc* with the muscle and aponeurotic tissues and the sample was taken centered on the linea alba. The heterogeneity and the multi-layered nature of the samples might prevent the observation of slight changes. Immunochemistry or histological analyses may improve the understanding of the healing behavior around the meshes: the prosthesis implantation involves a cellular and tissue remodeling that might explain why and how the mechanical properties of the composite adapt and change.

The animal model is the other main limitation of this study. The implantation on the abdominal wall is questionable: it cannot be representative of POP clinical cases. The animal model with vaginal implantation is probably better for tolerance. Regarding the mechanical properties no animal model, except non-human primate whose access is very limited access and expensive, presents a standing position, thus the mechanical constraints on the implants are also far from the human case. The abdominal wall model is imperfect but probably the most accessible and the closest that can be obtained. Implantations in an abdominal or vaginal environment were compared in rabbit [31, 32] and sheep model [33, 34]. In the sheep model, it seems that higher contraction or erosion rates happen in vaginal implantation, differences from an histological point of view are also noted. In a rabbit model, Ozog et al. [31] told about the technical difficulties of the vaginal implantation in a small animal model, preventing them to perform biomechanical observations. The rat model is still widely used in POP meshes studies and was however sufficient to study the impact of the mesh implantation on the mechanical properties of the native tissues. The surgical procedure could be slightly improved by using a defect model [35–38] in order to get closer to clinical cases and induce stronger healing constraints on the native tissues. However, a defect model on rats would still be closer to a hernia model than a genital prolapse model. For further investigation of the impact of the mesh in more representative conditions, ewes represent an interesting anatomical model [39], allowing for implantation on the vaginal wall. This model is already often used for the clinical and mechanical observations of POP meshes *in vivo* [40, 41].

In this study, the passive mechanical properties of the biological composites were tested, using quasi-static testing conditions. However, pelvic organs contain smooth muscles that contract *in vivo*. By extension, the meshes should also undergo contractions. A few studies have already considered this aspect in the characterization of the human or animal pelvic tissues [42, 43]. Coupled passive and active characterization of explants were also studied with commercial meshes [33, 44–46]. In Feola et al. [33] study, it seems that the contractile response after the stimulation with KCl solution of the underlying tissue tends to decrease after

the implantation of a commercial mesh. Hympánová et al. [46] assessed the contractility before and after the implantation without seeing a significant change with control tissue. Testing the biological composite in its active state, *ie* subjected to external stimulation could be an interesting development to better assess the compatibility of a mesh.

Non-resorbable meshes are supposed to stay permanently in the body and provide adapted support to the pelvic area while restoring the comfort of the patient in her everyday life. To promote its integration into the body, it seems preferable that the mesh should be able to correctly mimic the physiological behavior of the native tissues while preventing the reappearance or progression of the pathology. Meshes should be designed with regards to their *in vivo* role rather than the only specification on their raw properties.

Recent works [13, 47] stressed the importance of the biomechanical compatibility of the mesh implant. Unlike what the pathological extreme mobilities intuitively suggest, prolapsed tissues appear to be stiffer than non-pathological ones [48] as shown in Figure 8. Physiological deformations correspond to the area where stress and strain are considered as low, with respect to extreme or damaging zone [25]. This region is preserved in prolapsed tissues [48], Figure 8, and ensures the comfort of the patient in everyday life functions. Even if the location of the physiological range is not precisely defined and may slightly vary from ours, Mazza and Ehret [13] suggested similarly that compatible graft once implanted should mimic the mechanical properties of the native tissues in the physiological range.

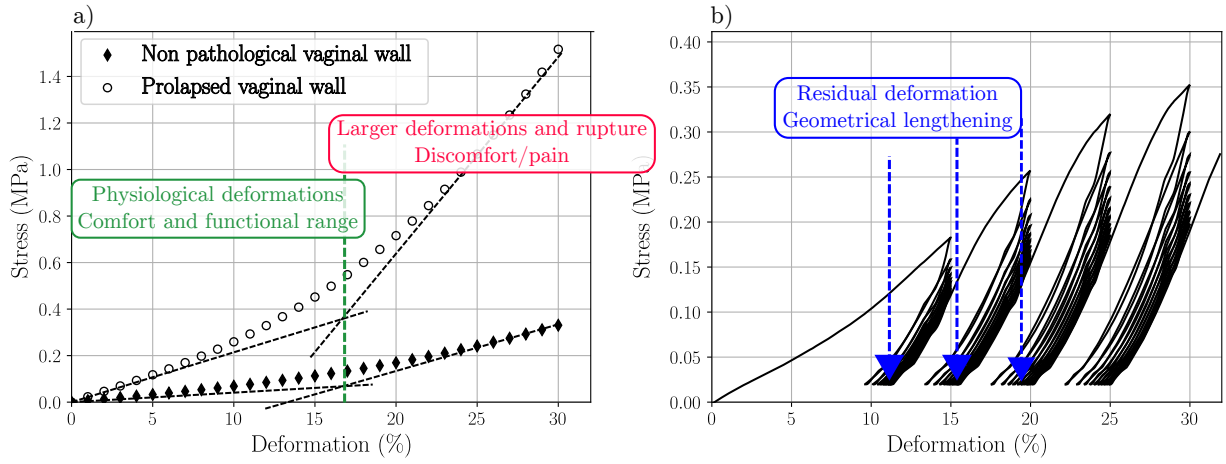

Figure 8: a) Mechanical response of the non-pathological and prolapsed vaginal wall [48]. The behavior is non-linear and presents two main regions: one where stress and strain remain low, the second is associated with higher stress, and severe damaging or rupture of the tissue. The first region corresponds to the physiological range where the organs function in everyday life. In the second region, the risk of pains and discomforts are higher due to larger stresses. Round and diamond markers indicate respectively the experimental behavior of the pathological and non-pathological vaginal wall. Black dashed lines illustrate the tangent behavior in small and large deformations, respectively controlled by C_0 and C_1. The vertical green dashed line localizes the limit of the comfort zone. b) Typical mechanical response to cyclic loading of the human vaginal sample. Residual deformations, highlighted with the blue arrows, appear after the first cycles and increase over repeated loading.

Pelvic tissues also present a damageable response when cyclically loaded [49, 50] that may cause over time and repeated loadings increasing residual deformations, *ie* a geometrical lengthening of the tissues, see Figure 8. Numerical simulations [51] showed that this lengthening of the pelvic tissues has a stronger influence on POP occurrence than the change of the mechanical properties. Although it has never been fully investigated to our knowledge, these observations seem consistent with the clinical experience: surgeons often happen to resect tissues during POP surgery. Besides, Luo et al. [52] have also observed with MRI that the pelvic ligaments were significantly longer in prolapsed cases in comparison with non-prolapsed ones.

Meshes should help to restore the anatomy and physiological functions of the pelvic area. Implanted meshes should, therefore, be designed and tested to match the mechanical behavior of the native tissue. Prolapsed tissues are already stiffer [48] than non prolapsed ones, the stiffness increase does not seem to

prevent the occurrence of POP. Geometrical observations [51, 52] suggest that the lengthening of pelvic structures might be a cause of its apparition. One can, therefore, assume that the mesh should preferably not stiffen the pelvic system but rather protect the native tissues from being exposed to extreme deformations that would cause important residual deformation and geometrical lengthening. It also seems that the optimal mesh should not shrink the physiological deformation range: it would create higher, non-physiological stresses in the pelvic tissue, thus pain or discomfort to the patients.

Beyond the mechanical rigidities and stress-strain response shape, the present study aims at pointing the role of the mesh from other mechanical aspects. Instead of stiffening the native tissues, the optimal mesh should, therefore, preserve the physiological mechanical behavior of the native tissues and limit the progression of the natural lengthening to restore and ensure the physiological functions of the pelvic area.

The approach presented in this work allowed us to assess the compatibility and mechanical changes following mesh implantation. With respect to the mechanical behavior of the non-pathological pelvic system, mesh B appears at the time to achieve the best compromise between mechanical, clinical, and structural specifications. Choosing the best candidate in this study remains challenging, demanding an important testing process that involved an animal study. Unfortunately the limitations of this study (implantation location, low number of animals,...) prevent us to fully demonstrate if the mesh B is a suitable candidate for the cure of POP. Extensive studies are still required to better determine the link between the mesh's architecture and its mechanical properties before implantation and the clinical outcomes as well as mechanical impact after implantation. Mechanical observations could be combined with histological considerations in a representative animal model. More generally, understanding the changes due to implantation as well as the impact of the textile's architecture could help in faster and safer meshes design.

Conclusion

Whatever route for implantation is chosen, new and well-adapted meshes are required to improve the cure of POP. Pore size, shape, density, or even mechanical properties of the raw textile could not be alone predictive of the implantation results.

The mesh once implanted can condition three mechanical aspects of the native tissues: rigidities, comfort zone, and residual deformation. Residual deformations, caused by repeated solicitation lead to a geometrical lengthening of the native tissues and are believed to be a reason for the apparition of prolapse. Meshes could yet help in restoring the pelvic static and inhibit the relapse risk. Reducing the range of the comfort zone could cause severe pain and discomfort to the patient. Instead of stiffening the native tissues, the optimal mesh should preserve the physiological mechanical behavior of the native tissues and limit the progression of the natural lengthening to restore and ensure the physiological functions of the pelvic area.

Three meshes and their *in vivo* effect after implantation were compared. One mesh seems to provide more adequate support and mechanical biocompatibility, with both better clinical results in terms of postoperative complications and a more physiological mechanical response. Further extensive studies are required to better understand the link between *ex* and *in vivo* mechanical properties and extrapolate the results in anatomically representative conditions.

Acknowledgments

The authors thanks the French National Research Agency (ANR-13-TECS-0003-01) for the financial funding of this study.

This work is part of PROBIOMESH, an Interreg France-Wallonie-Vlaanderen project supported by the European Regional Development Fund.

The authors wish to thank Franois Lesaffre for the design and development of the testing machine Biotens, Pauline Lecomte-Grosbras and Jean-François Witz who helped during the analysis of the experimental results, Bram Pouseele and Lilia Bougherara who assisted Dr Doucède during the implantation phases.

References

[1] Aqsa A. Khan, Karyn S. Eilber, J. Quentin Clemens, Ning Wu, Chris L. Pashos, and Jennifer T. Anger. Trends in management of pelvic organ prolapse among female Medicare beneficiaries. American Journal of Obstetrics and Gynecology, 212(4):463.e1–463.e8, 2015. ISSN 10976868. doi: 10.1016/j.ajog.2014.10.025. URL http://dx.doi.org/10.1016/j.ajog.2014.10.025.

[2] Lisa Rogo-Gupta, Larissa V. Rodriguez, Mark S. Litwin, Thomas J. Herzog, Alfred I. Neugut, Yu-Shiang Lu, Shlomo Raz, Dawn L. Hershman, and Jason D. Wright. Trends in surgical mesh use for pelvic organ prolapse from 2000 to 2010. Obstetrics and gynecology, 120(5):1105–15, 2012. ISSN 1873-233X. doi: http://10.1097/AOG.0b013e31826ebcc2. URL http://www.ncbi.nlm.nih.gov/pubmed/23090529.

[3] Christopher Maher, Benjamin Feiner, Kaven Baessler, Corina Christmann-Schmid, Nir Haya, and Jane Marjoribanks. Transvaginal mesh or grafts compared with native tissue repair for vaginal prolapse. Cochrane Database of Systematic Reviews, 2016(2):10–13, 2016. ISSN 13616137. doi: 10.1002/14651858.CD012079.

[4] Virginie Bot-Robin, Jean-Philippe Lucot, Géraldine Giraudet, Chrystèle Rubod, and Michel Cosson. Use of vaginal mesh for pelvic organ prolapse repair: a literature review. Gynecological Surgery, 9(1):3–15, sep 2011. ISSN 1613-2076. doi: 10.1007/s10397-011-0702-8. URL http://dx.doi.org/10.1007/s10397-011-0702-8http://link.springer.com/10.1007/s10397-011-0702-8.

[5] Husam Abed, David D. Rahn, Lior Lowenstein, Ethan M. Balk, Jeffrey L. Clemons, and Rebecca G. Rogers. Incidence and management of graft erosion, wound granulation, and dyspareunia following vaginal prolapse repair with graft materials: A systematic review, 2011. ISSN 09373462.

[6] Loïc Boulanger, Malik Boukerrou, Eric Lambaudie, André Defossez, and Michel Cosson. Tissue integration and tolerance to meshes used in gynecologic surgery: An experimental study. Eur. J. Obstet. Gynecol. Reprod. Biol., 125(1):103–108, mar 2006. ISSN 0301-2115. doi: http://dx.doi.org/10.1016/j.ejogrb.2005.07.029. URL http://www.sciencedirect.com/science/article/pii/S0301211505004136http://www.ncbi.nlm.nih.gov/pubmed/16169657.

[7] Audra Jolyn Hill, Cecile A Unger, Ellen R Solomon, Jennifer A Brainard, and Matthew D Barber. Histopathology of excised midurethral sling mesh. Int. U, 26:591–595, 2015. doi: 10.1007/s00192-014-2553-0.

[8] Alexis L Nolfi, Bryan N Brown, Rui Liang, Stacy L Palcsey, Michael J Bonidie, Steven D Abramowitch, and Pamela A Moalli. Host response to synthetic mesh in women with mesh complications. The American Journal of Obstetrics & Gynecology, 215(2):206.e1–206.e8, 2016. ISSN 0002-9378. doi: 10.1016/j.ajog.2016.04.008. URL http://dx.doi.org/10.1016/j.ajog.2016.04.008.

[9] P. K. Amid. Classification of biomaterials and their related complications in abdominal wall hernia surgery. Hernia, 1: 15–21, 1997.

[10] Michel Cosson, Philippe Debodinance, Malik Boukerrou, M. P. Chauvet, Pierre Lobry, Gilles Crépin, and Anne Ego. Mechanical properties of synthetic implants used in the repair of prolapse and urinary incontinence in women: which is the ideal material? International urogynecology journal and pelvic floor dysfunction, 14(3):169–78, aug 2003. ISSN 0937-3462. doi: 10.1007/s00192-003-1066-z. URL http://www.ncbi.nlm.nih.gov/pubmed/12955338http://dx.doi.org/10.1007/s00192-003-1066-z.

[11] R. Liang, S. Abramowitch, K. Knight, S. Palcsey, A. Nolfi, Andrew Feola, S. Stein, and Pamela A. Moalli. Vaginal degeneration following implantation of synthetic mesh with increased stiffness. BJOG : an international journal of obstetrics and gynaecology, 120(2):233–43, jan 2013. ISSN 1471-0528. doi: 10.1111/1471-0528.12085. URL http://dx.doi.org/10.1111/1471-0528.12085http://www.pubmedcentral.nih.gov/articlerender.fcgi?artid=3531826{&}tool=pmcentrez{&}rendertype=abstracthttp://www.pubmedcentral.nih.gov/articlerender.fcgi?artid=3531826{%}7B{&}{%}7Dtool=pmcentrez{%}7B{&}{%}7Drendertype=abstract.

[12] Boris Gabriel, Chrystèle Rubod, Mathias Brieu, Bruno Dedet, Laurent de Landsheere, Vincent Delmas, and Michel Cosson. Vagina, abdominal skin, and aponeurosis: do they have similar biomechanical properties ? International Urogynecology Journal, 22(1):23–7, jan 2011. ISSN 1433-3023. doi: 10.1007/s00192-010-1237-7. URL http://www.ncbi.nlm.nih.gov/pubmed/20798926http://dx.doi.org/10.1007/s00192-010-1237-7.

[13] Edoardo Mazza and Alexander E. Ehret. Mechanical biocompatibility of highly deformable biomedical materials. Journal of the Mechanical Behavior of Biomedical Materials, 48:100–124, aug 2015. ISSN 17516161. doi: 10.1016/j.jmbbm.2015.03.023. URL http://linkinghub.elsevier.com/retrieve/pii/S1751616115001046http://www.sciencedirect.com/science/article/pii/S1751616115001046.

[14] A. Feola, S. Abramowitch, Z. Jallah, S. Stein, W. Barone, S. Palcsey, and P. Moalli. Deterioration in biomechanical properties of the vagina following implantation of a high-stiffness prolapse mesh. BJOG: An International Journal of Obstetrics & Gynaecology, 120(2):224–232, jan 2013. ISSN 1471-0528. doi: 10.1111/1471-0528.12077. URL http://dx.doi.org/10.1111/1471-0528.12077http://www.pubmedcentral.nih.gov/articlerender.fcgi?artid=3530836{%}7B{&}{%}7Dtool=pmcentrez{%}7B{&}{%}7Drendertype=abstracthttp://www.pubmedcentral.nih.gov/articlerender.fcgi?artid=3530836{%}7B{%}25{%}7D7B{%}7B{&}{%}7D{%}7B{%}25{%}7D7Dtool=phttp://www.pubmedcentral.nih.gov/articlerender.fcgi?artid=3530836{&}tool=pmcentrez{&}rendertype=abstract.

[15] Yves Ozog, M. L. Konstantinovic, Erika Werbrouck, D. De Ridder, Edoardo Mazza, and Jan Deprest. Persistence of polypropylene mesh anisotropy after implantation: an experimental study. BJOG: An International Journal of Obstetrics & Gynaecology, 118(10):1180–1185, 2011. ISSN 1471-0528. doi: 10.1111/j.1471-0528.2011.03018.x. URL http://dx.doi.org/10.1111/j.1471-0528.2011.03018.x.

[16] B. Hernández-Gascón, E. Peña, G. Pascual, M. Rodríguez, J. M. Bellón, and B. Calvo. Long-term anisotropic mechanical response of surgical meshes used to repair abdominal wall defects. Journal of the Mechanical Behavior of Biomedical

Materials, 5(1):257–71, jan 2012. ISSN 1878-0180. doi: 10.1016/j.jmbbm.2011.09.005. URL http://www.sciencedirect.com/science/article/pii/S1751616111002396.

[17] J M Bellon, M Rodriguez, N Garcia-Honduvilla, V Gomez-Gil, G Pascual, and J Bujan. Comparing the Behavior of Different Polypropylene Meshes (Heavy and Lightweight) in an Experimental Model of Ventral Hernia Repair. Journal of Biomedical Materials Research, 89B(2):448–455, 2009. doi: 10.1002/jbm.b.31234.

[18] Sharon L. Edwards, Jerome A. Werkmeister, Anna Rosamilia, John A. M. Ramshaw, Jacinta F. White, and Caroline E. Gargett. Characterisation of clinical and newly fabricated meshes for pelvic organ prolapse repair. Journal of the Mechanical Behavior of Biomedical Materials, 23(0):53–61, jul 2013. ISSN 1751-6161. doi: http://dx.doi.org/10.1016/j.jmbbm.2013.04.002. URL http://www.sciencedirect.com/science/article/pii/S1751616113001239http://www.ncbi.nlm.nih.gov/pubmed/23651550.

[19] A. Morch, B. Pouseele, G. Doucède, J.-F. Witz, F. Lesaffre, P. Lecomte-Grosbras, M. Brieu, M. Cosson, and C. Rubod. Experimental study of the mechanical behavior of an explanted mesh: The influence of healing. Journal of the Mechanical Behavior of Biomedical Materials, 65:190–199, 2017. ISSN 18780180. doi: 10.1016/j.jmbbm.2016.07.033.

[20] G. Doucède, A. Morch, B. Pouseele, P. Lecomte-Grosbras, M. Brieu, M. Cosson, and C. Rubod. Evolution of the mechanical properties of a medical device regarding implantation time. European Journal of Obstetrics & Gynecology and Reproductive Biology, 242:139–143, 2019.

[21] Hans Peter Dietz, Max Erdmann, and Ka Lai Shek. Mesh contraction: myth or reality? American Journal of Obstetrics and Gynecology, 204(2):173.e1—-173.e4, feb 2011. ISSN 0002-9378. doi: http://dx.doi.org/10.1016/j.ajog.2010.08.058. URL http://www.sciencedirect.com/science/article/pii/S0002937810011130http://www.ncbi.nlm.nih.gov/pubmed/20965481.

[22] O. H. Yeoh. Some forms of the strain energy function for rubber. Rubber Chemistry and Technology, 66(5):754–771, 1993. doi: 10.5254/1.3538343. URL http://dx.doi.org/10.5254/1.3538343.

[23] Eric Jones, Travis Oliphant, and Pearu Peterson. SciPy : Open source scientific tools for Python, 2001. URL http://www.scipy.org/.

[24] Alejandra M Ruiz-zapata, Andrew J Feola, John Heesakkers, and Petra De Graaf. Biomechanical Properties of the Pelvic Floor and its Relation to Pelvic Floor Disorders. European Urology Supplements, 17(3):80–90, 2018. ISSN 1569-9056. doi: 10.1016/j.eursup.2017.12.002. URL http://dx.doi.org/10.1016/j.eursup.2017.12.002.

[25] Yves Ozog, Maja L. Konstantinovic, Erika Werbrouck, Dirk De Ridder, Mazza Edoardo, and Jan Deprest. Shrinkage and biomechanical evaluation of lightweight synthetics in a rabbit model for primary fascial repair. International Urogynecology Journal, 22(9):1099–1108, sep 2011. ISSN 0937-3462. doi: 10.1007/s00192-011-1440-1. URL http://dx.doi.org/10.1007/s00192-011-1440-1http://www.ncbi.nlm.nih.gov/pubmed/21562913.

[26] U. Klinge and B. Klosterhalfen. Modified classification of surgical meshes for hernia repair based on the analyses of 1,000 explanted meshes. Hernia, 16:251–258, 2012. ISSN 12654906. doi: 10.1007/s10029-012-0913-6.

[27] Spencer P. Lake, Shuddhadeb Ray, Ahmed M. Zihni, Dominic M. Thompson, Jeffrey Gluckstein, and Corey R. Deeken. Pore size and pore shape–but not mesh density–alter the mechanical strength of tissue ingrowth and host tissue response to synthetic mesh materials in a porcine model of ventral hernia repair. Journal of the Mechanical Behavior of Biomedical Materials, 42:186–97, feb 2015. ISSN 1878-0180. doi: 10.1016/j.jmbbm.2014.11.011. URL http://www.sciencedirect.com/science/article/pii/S1751616114003634.

[28] B. Röhrnbauer and Edoardo Mazza. Uniaxial and biaxial mechanical characterization of a prosthetic mesh at different length scales. Journal of the Mechanical Behavior of Biomedical Materials, 29(0):7–19, jan 2014. ISSN 1751-6161. doi: http://dx.doi.org/10.1016/j.jmbbm.2013.07.021. URL http://www.sciencedirect.com/science/article/pii/S1751616113002543http://www.ncbi.nlm.nih.gov/pubmed/24041753.

[29] L. Melman, E. D. Jenkins, N. A. Hamilton, L. C. Bender, M. D. Brodt, C. R. Deeken, S. C. Greco, M. M. Frisella, and B. D. Matthews. Histologic and biomechanical evaluation of a novel macroporous polytetra. Hernia, 15:423–431, 2011. doi: 10.1007/s10029-011-0787-z.

[30] Daniela Ulrich, Sharon L. Edwards, David L.J. J. Alexander, Anna Rosamilia, Jerome A. Werkmeister, Caroline E. Gargett, and Vincent Letouzey. Changes in pelvic organ prolapse mesh mechanical properties following implantation in rats. American Journal of Obstetrics and Gynecology, 214(2):260.e1–260.e8, 2016. ISSN 10976868. doi: 10.1016/j.ajog.2015.08.071. URL http://www.sciencedirect.com.insis.bib.cnrs.fr/science/article/pii/S0002937815010194.

[31] Yves Ozog, Edoardo Mazza, Dirk Ridder, Jan Deprest, Dirk De Ridder, Jan Deprest, and Dirk Ridder. Biomechanical effects of polyglecaprone fibers in a polypropylene mesh after abdominal and rectovaginal implantation in a rabbit. International Urogynecology Journal, 23(10):1397–1402, oct 2012. ISSN 0937-3462. doi: 10.1007/s00192-012-1739-6. URL http://dx.doi.org/10.1007/s00192-012-1739-6http://www.ncbi.nlm.nih.gov/pubmed/22527542.

[32] Xuemei Fan, Yanzhou Wang, Yu Wang, and Huicheng Xu. Comparison of polypropylene mesh and porcine-derived , cross-linked urinary bladder matrix materials implanted in the rabbit vagina and abdomen. Int. Urogynecol. J., 25:683–689, 2014. doi: 10.1007/s00192-013-2283-8.

[33] Andrew Feola, Masayuki Endo, Iva Urbankova, Thomas Deprest, Samantha Bettin, Bernd Klosterhalfen, Jan Deprest, Avaulta Solo, Bard Medical, and Sofradim International. Host reaction to vaginally inserted collagen containing polypropylene implants in sheep. Am. J. Obstet. Gynecol., 212(April):474.e1–8, 2015. doi: 10.1016/j.ajog.2014.11.008.

[34] S Manodoro, M Endo, P Uvin, M Albersen, J Vlacil, A Engels, B Schmidt, A Feola, D De Ridder, and J Deprest. Graft-related complications and biaxial tensiometry following experimental vaginal implantation of flat mesh of variable dimensions. BJOG, 120:244–250, 2013. doi: 10.1111/1471-0528.12081.

[35] U. Klinge, V. Schumpelick, and B. Klosterhalfen. Functional assessment and tissue response of short- and long-term absorbable surgical meshes. Biomaterials, 22(11):1415–1424, 2001. ISSN 01429612. doi: 10.1016/S0142-9612(00)00299-4.

[36] Maja L. Konstantinovic, Eline Pille, Marta Malinowska, Eric Verbeken, Dirk Ridder, and Jan Deprest. Tensile strength

and host response towards different polypropylene implant materials used for augmentation of fascial repair in a rat model. International Urogynecology Journal and Pelvic Floor Dysfunction, 18(6):619–626, 2007. ISSN 09373462. doi: 10.1007/s00192-006-0202-y.

[37] Daniela Ulrich, Sharon L. Edwards, Jacinta F. White, Tommy Supit, John A. M. Ramshaw, Camden Lo, Anna Rosamilia, Jerome A. Werkmeister, and Caroline E. Gargett. A Preclinical Evaluation of Alternative Synthetic Biomaterials for Fascial Defect Repair Using a Rat Abdominal Hernia Model. PLoS ONE, 7(11), 2012. ISSN 19326203. doi: 10.1371/journal.pone.0050044.

[38] Lucie Hympanova, Marina Gabriela Monteiro Carvalho Mori da Cunha, Rita Rynkevic, Manuel Zündel, Monica Ramos Gallego, Jakob Vange, Geertje Callewaert, Iva Urbankova, Frank Van der Aa, Edoardo Mazza, and Jan Deprest. Physiologic musculofascial compliance following reinforcement with electrospun polycaprolactone-ureidopyrimidinone mesh in a rat model. Journal of the Mechanical Behavior of Biomedical Materials, 74(June):349–357, 2017. ISSN 18780180. doi: 10.1016/j.jmbbm.2017.06.032. URL http://dx.doi.org/10.1016/j.jmbbm.2017.06.032.

[39] Iva Urbankova and Rita Rynkevic. Comparative Anatomy of the Ovine and. 2017. doi: 10.1159/000454771.

[40] Renaud De Tayrac, Antoine Alves, and Michel Thérin. Collagen-coated vs noncoated low-weight polypropylene meshes in a sheep model for vaginal surgery . A pilot study. pages 513–520, 2007. doi: 10.1007/s00192-006-0176-9.

[41] Masayuki Endo, Iva Urbankova, Jaromir Vlacil, Siddarth Sengupta, and Thomas Deprest. Cross-linked xenogenic collagen implantation in the sheep model for vaginal surgery. pages 113–122, 2015. doi: 10.1007/s10397-015-0883-7.

[42] Andrew Feola, Pamela M Moalli, Marianna Alperin, Robbie Duerr, R obin Gandley, and Steven Abramowitch. Impact of Pregnancy and Vaginal Delivery on the Passive and Active Mechanics of the Rat Vagina. Annals of Biomedical Engineering, 39(1):549–558, 2011. doi: 10.1007/s10439-010-0153-9.

[43] Alyssa Huntington, Emanuele Rizzuto, Steven Abramowitch, Zaccaria Del Prete, and Raffaella De Vita. Anisotropy of the Passive and Active Rat Vagina Under Biaxial Loading. Annals of Biomedical Engineering, 47(1):272–281, 2019. doi: 10.1007/s10439-018-02117-9.

[44] Andrew Feola, Robert Duerr, Pamela Moalli, and Steven Abramowitch. Changes in the rheological behavior of the vagina in women with pelvic organ prolapse. Int. Urogynecol. J., 24(7):1221–1227, jul 2013. ISSN 0937-3462. doi: 10.1007/s00192-012-2002-x. URL http://dx.doi.org/10.1007/s00192-012-2002-xhttp://www.ncbi.nlm.nih.gov/pubmed/23208004.

[45] Z Jallah, R Liang, A Feola, W Barone, S Palcsey, S D Abramowitch, and N Yoshimura. The impact of prolapse mesh on vaginal smooth muscle structure and function. BJOG, 123:1076–1085, 2016. doi: 10.1111/1471-0528.13514.

[46] Lucie Hympánová, Rita Rynkevic, Sabiniano Román, Marina G.M.C. Mori da Cunha, Edoardo Mazza, Manuel Zündel, Iva Urbánková, Monica R. Gallego, Jakob Vange, Geertje Callewaert, Christopher Chapple, Sheila MacNeil, and Jan Deprest. Assessment of Electrospun and Ultra-lightweight Polypropylene Meshes in the Sheep Model for Vaginal Surgery. European Urology Focus, 2018. ISSN 24054569. doi: 10.1016/j.euf.2018.07.024.

[47] M. M. Maurer, B. Röhrnbauer, A. Feola, J. Deprest, and E. Mazza. Mechanical biocompatibility of prosthetic meshes: A comprehensive protocol for mechanical characterization. Journal of the Mechanical Behavior of Biomedical Materials, 40:42–58, aug 2014. ISSN 17516161. doi: 10.1016/j.jmbbm.2014.08.005. URL http://www.sciencedirect.com/science/article/pii/S1751616114002483.

[48] Clay Jean-Charles, Chrystèle Rubod, Mathias Brieu, Malik Boukerrou, Jean Fasel, Michel Cosson, Jean-Charles Clay, Chrystèle Rubod, Mathias Brieu, Malik Boukerrou, Jean Fasel, and Michel Cosson. Biomechanical properties of prolapsed or non-prolapsed vaginal tissue: impact on genital prolapse surgery. Int. Urogynecol. J., 21(12):1535–8, dec 2010. ISSN 1433-3023. doi: 10.1007/s00192-010-1208-z. URL http://dx.doi.org/10.1007/s00192-010-1208-zhttp://www.ncbi.nlm.nih.gov/pubmed/20838989.

[49] Chrystèle Rubod, Mathias Brieu, Michel Cosson, Géraldine Rivaux, Jean-Charles Clay, Laurent de Landsheere, and Boris Gabriel. Biomechanical properties of human pelvic organs. Urology, 79(4):968.e17–968.e22, apr 2012. ISSN 0090-4295. doi: http://dx.doi.org/10.1016/j.urology.2011.11.010. URL http://www.ncbi.nlm.nih.gov/pubmed/22245302http://www.sciencedirect.com/science/article/pii/S0090429511026331.

[50] Estefania Peña, P. Martins, Teresa Mascarenhas, R. M. Natal Jorge, A. Ferreira, M. Doblaré, and B. Calvo. Mechanical characterization of the softening behavior of human vaginal tissue. Journal of the Mechanical Behavior of Biomedical Materials, 4(3):275–283, apr 2011. ISSN 1751-6161. doi: http://dx.doi.org/10.1016/j.jmbbm.2010.10.006. URL http://www.sciencedirect.com/science/article/pii/S175161611000144Xhttp://www.ncbi.nlm.nih.gov/pubmed/21316615.

[51] Olivier Mayeur, Gery Lamblin, Pauline Lecomte-Grosbras, Mathias Brieu, Chrystele Rubod, and Michel Cosson. FE simulation for the understanding of the median cystocele prolapse occurrence. Biomedical Simulation, 44:220–227, 2016. ISSN 16113349. doi: 10.1007/978-3-319-12057-7_25. URL http://link.springer.com/10.1007/978-3-319-12057-7{_}25.

[52] Jiajia Luo, Cornelia Betschart, Luyun Chen, J. A. Ashton-Miller, and John O.L. DeLancey. Using stress MRI to analyze the 3D changes in apical ligament geometry from rest to maximal Valsalva: a pilot study. Int. Urogynecol. J., 25(2):197–203, 2014. doi: 10.1007/s00192-013-2211-y.Using.